

New Directions for Atomic Steps: Step Alignment by Grazing Incident Ion Beams on TiO₂(110)

Tim Luttrell,¹ Wei-Kun Li,² Xue-Qing Gong,^{2,*} and Matthias Batzill^{1,*}

¹*Department of Physics, University of South Florida, Tampa, Florida 33620, USA*

²*Labs for Advanced Materials, Research Institute of Industrial Catalysis, East China University of Science and Technology, 130 Meilong Road, Shanghai 200237, People's Republic of China*

(Received 21 January 2009; published 22 April 2009)

Grazing incidence low energy ion beams preferentially erode steps with directional components normal to the azimuthal direction of the beam, thus generating step edges aligned along the beam direction. With this kinetic method, the fabrication of thermodynamically metastable low index step-edge orientations is demonstrated on TiO₂(110). The $\langle 1\bar{1}0 \rangle$ step edge is prepared, enabling its atomic structure determination by scanning tunneling microscopy and density-functional theory. A reconstructed atom configuration is revealed, which is reminiscent of the structure of the rutile-TiO₂(001)-(2 × 1) face.

DOI: 10.1103/PhysRevLett.102.166103

PACS numbers: 68.47.Gh, 61.80.Jh, 68.35.B-, 68.35.Md

The properties of monatomic-height steps are central for many processes at surfaces, such as etching [1], nucleation [2], and chemical reaction [3]. Step edges with different crystallographic orientations exhibit specific electronic [4] and chemical properties [5]. Consequently, controlling step-edge orientations enables tuning of interface functionalities. Although any step orientation can be theoretically constructed, energy minimization during heat treatment prevents formation of most step orientations.

Low energy ion beams have been successfully employed for the preparation of thin films with a preferred texture [6]. In this method, the ion beam destabilizes grains with high sputter yield resulting from an unfavorable crystallographic orientation relative to the ion beam. Here, this principle of creating a texture by preferential removal of structures with a high sputter yield is extended from 3D films to 2D surfaces. In particular, variations in the sputter yield of step edges as a function of their orientations relative to a grazing incident ion beam are exploited to form step-edge textures with a preferential alignment of steps parallel to the beam. More importantly, we show that with this technique, steps that are thermodynamically disfavored can be kinetically stabilized. We demonstrate this method by preparing and characterizing the thermodynamically metastable $\langle 1\bar{1}0 \rangle$ step on rutile-TiO₂(110).

All the experiments were performed in an ultra high vacuum (UHV) chamber equipped with a commercial low energy ion gun and a variable temperature STM. All samples were irradiated at a polar angle of $83.0 \pm 0.5^\circ$ measured from the surface normal with an Ar⁺ ion beam of 0.8 keV along low index azimuth-directions of the substrate. The TiO₂ substrates were oriented in the (110) orientation and STM images of freshly prepared samples showed terraces 10–30 nm wide. During irradiation, the sample temperature was kept at 400 °C if not noted otherwise. Empty-state STM measurements were performed *in situ* with a bias voltage of 1.5 V and tunnel current of ~1 nA.

For assessing the stability of step-edge structures and to interpret STM images, total energy density-functional theory (DFT) calculations have been carried out within the generalized gradient approximation (GGA) using the PWSCF code included in the QUANTUM-ESPRESSO package [7]. Electron-ion interactions were described by ultrasoft pseudopotentials [8], with electrons from O 2*s*, 2*p*, and Ti 3*s*, 3*p*, 3*d*, 4*s* shells explicitly included in the calculations. Plane-wave basis set cutoffs for the smooth part of the wave functions and the augmented density were 25 and 200 Ry, respectively. The $\langle 1\bar{1}0 \rangle$ steps at rutile TiO₂(110) were modeled with vicinal rutile TiO₂(441) surface, which contains (110) terraces and monoatomic $\langle 1\bar{1}0 \rangle$ steps. A periodic slab with 4 layers of oxide was used and the vacuum between slabs is ~10 Å. In order to model the 2 × 1 reconstructed structure (see below), we also used a (2 × 1) surface cell with corresponding 2 × 2 × 1 *k*-point mesh. All the atoms within the slab were allowed to move in structural optimization (force threshold is 0.05 eV/Å). Simulated STM images were calculated within the Tersoff-Hamann approach [9], under empty-state conditions with a 1 eV energy window and a fixed distance of ~2 Å above the terrace twofold coordinated O O_{2c} [the cut-plane is parallel to the (110) facet].

It has been previously shown that the sputter yield of a grazing incidence low energy ion beam varies largely at flat terraces compared to defect sites such as step edges [10]. For low ion energies (~1 keV) and large incidence angles (larger than ~80°), ions may reflect from a terrace without penetrating the surface layer, and thus only limited kinetic sputtering of surface atoms occurs. Ions impacting close to a step edge, on the other hand, experience a locally steeper impact angle and thus cause sputter damage. Thus, ion sputtering at grazing angles is fundamentally different from sputtering at steeper angles. At steeper angles, the ions deposit their energy deeper in the bulk, and surface-curvature dependent sputter yields cause surface instabilities and pattern formation [11]. Figure 1(a) illustrates the localized nature of sputtering at step edges for a grazing

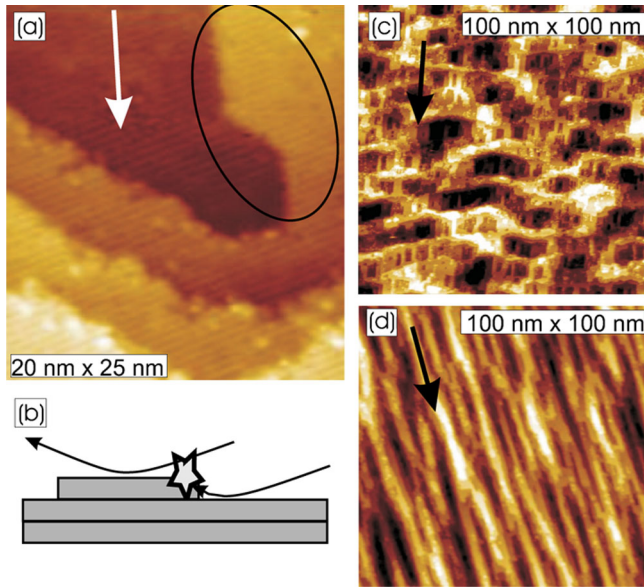


FIG. 1 (color online). STM images of atomic-height step edges irradiated with a grazing 0.8 keV Ar ion beam. (a) Details of sputter damage of step edges after irradiation at room temperature with very low ion fluence ($\sim 8 \times 10^{14}$ ions/cm²). The steps within the oval are not damaged because they are oriented parallel or are step-down edges relative to the ion beam. (b) Cartoon illustrating sputtering events at step-up edges and reflection of the ion beam from terraces. Surface structures after irradiating the sample at 400 °C with ion fluences of (c) 1.7×10^{16} ions/cm² and (d) 5.6×10^{16} ions/cm², respectively, with the ion beam azimuthal direction along the [001] crystallographic direction of the TiO₂(110) surface. The ion beam azimuth is indicated by arrows.

incident ion beam on a TiO₂(110) sample irradiated at room temperature. Sputter damage is mainly located along step edges that are facing the ion beam (step-up), thus demonstrating strong sputter-yield anisotropy under these experimental conditions. From the analogy of ion beam assisted film growth, it is thus expected that the surface arranges in a step texture that reduces the overall sputtering. This is accomplished by minimizing steps with a directional component normal to the ion beam. If sputtering was only limited to step edges, this would result in the erosion of all steps and eventually a stepless surface. Such a scenario is unrealistic though. Some sputtering at terrace sites will occur, e.g., at point defects, and ions impacting at step edges will induce sputter damage also at lower terraces and creating vacancies away from the step edge [10]. Agglomeration of these vacancies leads to nucleation of “holes,” causing formation of new step edges and thus a roughening of the surface with longer sputter time. Therefore, combination of preferential sputtering of step edges exposed to a grazing incidence ion beam together with the nucleation of new step edges will give rise to a self-formation of a nanostructured surface [10].

In this Letter, we explore to what extent control can be exerted over step-edge orientation by a low energy grazing

ion beam. Of particular interest is the possibility of creating steps that are only metastable and thus do not withstand high temperature treatments necessary in other preparation methods.

Rutile TiO₂(110) single crystals were used as the substrate for these studies. TiO₂(110) is a model system for transition metal oxide surfaces [12,13]. At room temperature, complex sputter defects will form, and the surface becomes disordered, the onset of which can be seen in Fig. 1. In addition, the lighter oxygen atoms are preferentially sputtered, resulting in a Ti-enriched surface. For rutile TiO₂, it is established that Ti-cations easily diffuse. Thus, at elevated temperatures, local sputter damage can heal, and excess Ti diffuses into the bulk. Studies on sputter reduced surfaces have shown that a temperature of 400–700 K is sufficient to reestablish a stoichiometric surface [14]. In addition, atom mobility at elevated temperatures allows forming low energy constellations at step edges. Consequently, the combination of preferential sputtering of steps exposed to the ion beam and formation of low energy step constellation results in a stepped surface with steps preferentially oriented along the ion beam azimuth as is shown in Figs. 1(c) and 1(d). While the formation of thermodynamically favored step edges, i.e., step-edge orientations that are part of a 2D Wulff construction of terraces [15], may be generally useful for nanostructuring of surfaces, the main goal is the fabrication of low index step edges that have a higher formation energy and thus are not present in a thermodynamic equilibrium terrace structure.

TiO₂(110) samples prepared by annealing in vacuum exhibit terraces that are bound by step edges along $\langle 001 \rangle$ and $\langle 1\bar{1}1 \rangle$ directions [12,16]. Steps along the low index $\langle 1\bar{1}0 \rangle$ direction are not observed. Figure 2(a) shows a STM image of this typical surface morphology. The preponderance of certain step orientations is a consequence of free energy minimization. Especially in ionic and covalent materials, the formation energy for step edges is strongly orientation dependent. An estimate of the relative formation energies for different low index step edges can be obtained from viewing step edges as microfacets of low index surfaces; i.e., low index step edges should correlate to the surface energy of the extended faces. Surface energies have been calculated for TiO₂, and therefore we can categorize the different step-edge orientations. The $\langle 001 \rangle$ step edge can be viewed as a $\{110\}$, the $\langle 1\bar{1}1 \rangle$ as a $\{101\}$, and the $\langle 1\bar{1}0 \rangle$ as a $\{001\}$ microfacet [see Figs. 2(b)–2(e)]. The surface energies for TiO₂ increase in the order of $\{110\} < \{101\} < \{001\}$ [17], and consequently this indicates that the $\langle 1\bar{1}0 \rangle$ step edge has the highest step energy among the low index steps on TiO₂(110). This is in agreement with the absence of $\langle 1\bar{1}0 \rangle$ steps on annealed TiO₂(110). Furthermore, the $\{001\}$ faces of rutile TiO₂ are known to reconstruct in a 2×1 structure consisting of $\{101\}$ facets [18]. This raises the question if the analogy between step edges and microfacets can be extended to reconstructed surfaces; i.e., does the $\langle 1\bar{1}0 \rangle$ step have a

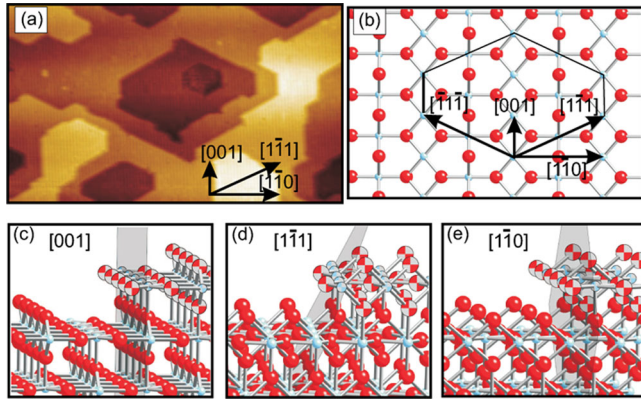


FIG. 2 (color online). Low energy step-edge structure on $\text{TiO}_2(110)$. (a) STM image of a typical surface structure of clean $\text{TiO}_2(110)$ surface, (b) orientations of the step edges on the surface (top view), and (c)–(e) illustrative structures of the different step edges (side views). In (c)–(e), the shaded area represents microfacets of an extended low index crystallographic plane corresponding to the step edge. Ti and O atoms are represented by small and big balls, respectively.

similar reconstruction as the extended $\{101\}$ face? In order to prepare and characterize the atomic scale structure of this high energy step edge, the grazing incident ion beam method is used. Figures 3(a) and 3(b) show STM images after grazing incidence ion irradiation along the $\langle 1\bar{1}0 \rangle$ azimuth. The majority of the step edges are now aligned with the direction of the ion beam. The thermal stability of this step orientation can be tested by annealing the sample for 5 min at ~ 900 K. After this heat treatment, the $\langle 1\bar{1}0 \rangle$ step edges convert into zigzagging steps with $\langle 1\bar{1}1 \rangle$ orientations, shown in Fig. 3(c). Although this increases the overall step-edge length, the small angle (24°) between the $\langle 1\bar{1}1 \rangle$ and the $\langle 1\bar{1}0 \rangle$ direction [see Fig. 2(b)] results in a length increase of only 10%. This increase in length has to be compensated for by an at least 10% lower formation energy for $\langle 1\bar{1}1 \rangle$ steps.

The preparation of high energy step edges enables the analysis of their atomic scale structure. A step-edge model is constructed from the measured periodicity of the step edge [twice that of the surface unit cell, see Fig. 3(b)] and invoking of charge counting arguments [19], i.e., creating a step edge that does not change the ratio of Ti/O atoms and thus allowing the cations and anions to retain their preferred nominal charges of $4+$ and $2-$, respectively. Such a step-edge model is shown in Figs. 4(a) and 4(b). This model consists of step segments with both $[1\bar{1}0]$ and $[1\bar{1}1]/[1\bar{1}\bar{1}]$ orientations and the step-edge Ti atoms are fourfold and fivefold coordinated compared to the sixfold bulk coordination. All the step-edge O atoms are twofold coordinated. To confirm this model, we performed *ab initio* DFT calculations to assess stability and atom relaxations at the step edge. We also calculated the unreconstructed $\langle 1\bar{1}0 \rangle$ step edge [Fig. 2(e)] for comparison. By assuming that their step-step interaction energies per unit area are identical, the step-edge formation energy was estimated to be

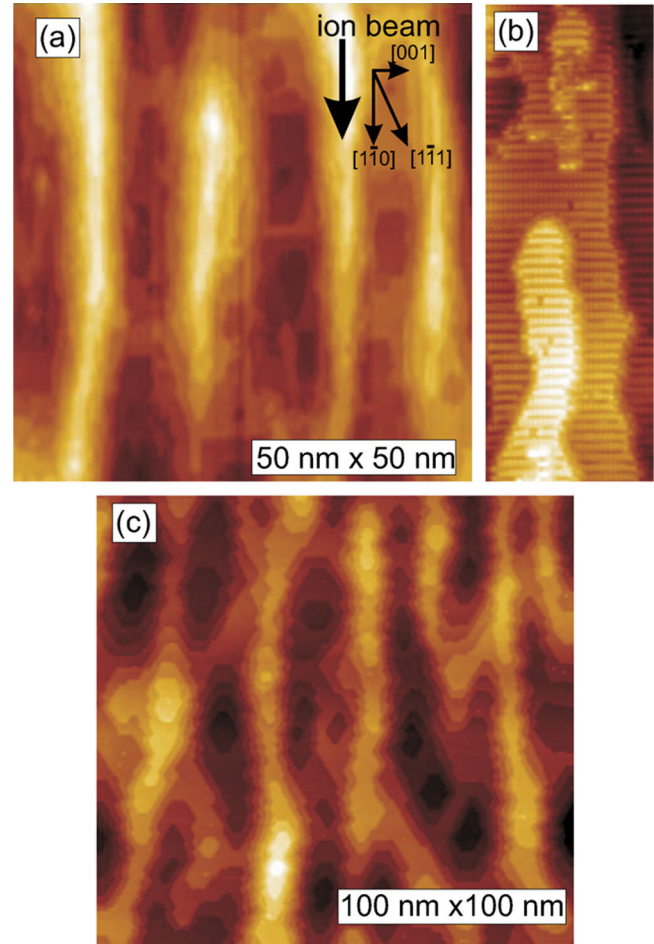


FIG. 3 (color online). Step edges fabricated by directing an ion beam along the $[1\bar{1}0]$ azimuth. The sample was irradiated with 0.8 keV Ar^+ ions with a total ion fluence of $\sim 5.6 \times 10^{16}$ ions/cm 2 . (a) Ridges formed on the surface along the ion beam azimuth, (b) atomic resolution of step edges along the $[1\bar{1}0]$ direction, and (c) the same sample as in (a) after annealing for 5 min at 900 K.

$0.09 \text{ eV}/\text{\AA}$ lower for the reconstructed step shown in Fig. 4. Moreover, the Tersoff-Hamann [9] plot of this step-edge structure is in excellent agreement with the experimental STM images as can be judged from Figs. 4(c) and 4(d). Therefore, the computational analysis corroborates this step-edge structure. The simulated STM images also reproduce the known fact that on terraces, the fivefold coordinated Ti (Ti_{5c}) atoms are imaged bright [12]. At the step edges, however, the twofold coordinated bridging oxygen atoms (O_{2c}) appear brighter under empty-state imaging conditions, indicating a variation of the tunneling probability for O_{2c} atoms on terraces compared to step edges. A similar effect has been observed for bridging twofold coordinated step-edge oxygen species on anatase $\text{TiO}_2(101)$ surfaces [15]. In both cases, the step-edge O_{2c} are coordinated to more under-coordinated Ti atoms. Apparently, this change in the local coordination environment of the O_{2c} has a pronounced effect on the empty orbitals and thus the STM contrast.

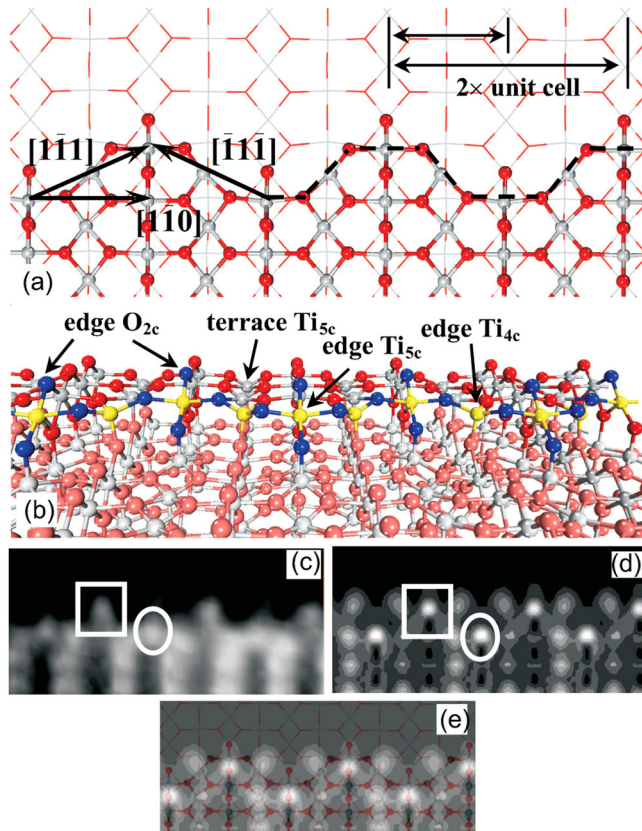


FIG. 4 (color online). Atomic scale structure of the $[1\bar{1}0]$ step edge. (a) and (b) Ball-and-stick models of the reconstructed step structure (top and side views, respectively). (c) Experimental STM image of step edge, (d) computed STM image, and (e) same as (d) superimposed on ball-and-stick model. In (a), the second-layer atoms are shown in thin lines, and in (b), they are shown in light tones. In (c) and (d), the squares and ovals specify the corresponding bright spots (edge O_{2c}) in experimental and simulated STM images.

It needs to be mentioned that there exists an interesting structural analogy between the extended $\{001\}$ face and the $\langle 1\bar{1}0 \rangle$ step-edge model. As mentioned above, the $\{001\}$ face reconstructs in a 2×1 structure consisting of $\{101\}$ facets. This (2×1) reconstruction for the extended face has the same atomic constellation as the proposed step-edge structure. This gives additional justification to the step-edge model and shows that viewing of step edges as facets of extended faces may also apply for certain surface reconstructions.

In conclusion, a grazing ion beam allows formation of high energy step edges that are thermally unstable. This allows access for studying the properties of these step edges. The ability of structuring single crystal substrates with high energy step edges may be utilized in model-catalyst studies for characterization of the chemical properties of these under-coordinated active sites, or for further processing of these surfaces by, for example, step-edge decoration [20], where high energy steps may exhibit

stronger adsorption sites. Finally, the success of directing surface features along an ion beam may point to a larger utility of grazing incidence low energy ion beams in surface preparation. For instance, symmetry breaking of multiple rotational domain structures (facets or reconstructions) by directing the beam along one domain symmetry direction seems possible.

The ECUST group acknowledges the financial support from National Natural Science Foundation of China (20703017) and the 111 project (B08021).

*Corresponding authors: xgong@ecust.edu.cn;

mbatzill@cas.usf.edu

- [1] J. Kasparian, M. Elwenspoek, and P. Allongue, *Surf. Sci.* **388**, 50 (1997).
- [2] E. J. Menke, Q. Li, and R. M. Penner, *Nano Lett.* **4**, 2009 (2004); X. Q. Gong *et al.*, *J. Am. Chem. Soc.* **130**, 370 (2008); A. Li *et al.*, *Phys. Rev. Lett.* **85**, 5380 (2000).
- [3] X. Q. Gong and A. Selloni, *J. Catal.* **249**, 134 (2007); C. Chizallet *et al.*, *J. Phys. Chem. B* **110**, 15878 (2006); S. C. Petitto, E. M. Malone, and M. A. Langell, *J. Phys. Chem. B* **110**, 1309 (2006).
- [4] L. Bartels *et al.*, *Phys. Rev. B* **67**, 205416 (2003).
- [5] M. M. Branda *et al.*, *J. Phys. Chem. C* **112**, 17643 (2008).
- [6] A. R. González-Elipé, F. Yubero, and J. M. Sanz, *Low Energy Ion Assisted Film Growth* (Imperial College Press, London, 2003).
- [7] S. Baroni, S. De Gironcoli, A. Dal Corso, and P. Giannozzi, *Quantum-Espresso*, <http://www.democritus.it>; J. P. Perdew, K. Burke, and M. Ernzerhof, *Phys. Rev. Lett.* **77**, 3865 (1996).
- [8] D. Vanderbilt, *Phys. Rev. B* **41**, 7892 (1990).
- [9] J. Tersoff and D. R. Hamann, *Phys. Rev. B* **31**, 805 (1985).
- [10] A. Friedrich and H. M. Urbassek, *Surf. Sci.* **547**, 315 (2003); A. Redinger *et al.*, *Phys. Rev. Lett.* **96**, 106103 (2006); A. Redinger *et al.*, *Phys. Rev. B* **77**, 195436 (2008).
- [11] T. Aste and U. Valbusa, *New J. Phys.* **7**, 122 (2005); A.-D. Brown and J. Erlebacher, *Phys. Rev. B* **72**, 075350 (2005); S. Park, B. Kahng, H. Jeong, and A.-L. Barabási, *Phys. Rev. Lett.* **83**, 3486 (1999); H. Zhou *et al.*, *Phys. Rev. B* **75**, 155416 (2007).
- [12] U. Diebold, *Surf. Sci. Rep.* **48**, 53 (2003).
- [13] A. Fujishima, X. Zhang, and D. A. Tryk, *Surf. Sci. Rep.* **63**, 515 (2008).
- [14] M. A. Henderson, *Surf. Sci.* **419**, 174 (1999).
- [15] X. Q. Gong *et al.*, *Nature Mater.* **5**, 665 (2006).
- [16] S. Fischer *et al.*, *Surf. Sci.* **337**, 17 (1995); H. Onishi, K.-I. Fukui, and Y. Iwasawa, *Bull. Chem. Soc. Jpn.* **68**, 2447 (1995); U. Diebold *et al.*, *Surf. Sci.* **411**, 137 (1998).
- [17] M. Ramamoorthy, D. Vanderbilt, and R. D. King-Smith, *Phys. Rev. B* **49**, 16721 (1994).
- [18] L. E. Firment, *Surf. Sci.* **116**, 205 (1982).
- [19] V. E. Henrich and S. K. Shaikhutdinov, *Surf. Sci.* **574**, 306 (2005).
- [20] F. J. Himpsel *et al.*, *MRS Bull.* **24**, 20 (1999).